Hindawi Publishing Corporation
International Journal of Antennas and Propagation
Volume 2013, Article ID 834387, 9 pages
http://dx.doi.org/10.1155/2013/834387

Research Article

Narrowband-to-Narrowband Frequency Reconfiguration with Harmonic Suppression Using Fractal Dipole Antenna

S. A. Hamzah, M. Esa, N. N. N. A. Malik, and M. K. H. Ismail

Department of Communication Engineering, UTM-MIMOS COE for Telecommunication Technology, Faculty of Electrical Engineering, Universiti Teknologi Malaysia, 81310 UTM Johor Bahru, Johor, Malaysia

Correspondence should be addressed to S. A. Hamzah; sahamzah@gmail.com

Received 4 January 2013; Revised 26 June 2013; Accepted 2 July 2013

Academic Editor: Tayeb A. Denidni

Harmonic suppressed fractal antenna with switches named TMFDB25 is developed to select desired frequency band from 400 MHz to 3.5 GHz. The radiating element length is changed to tune the operating frequency while the stub is used to eliminate the undesired harmonic frequency. The balun circuit is reduced by 75% from the original size. The antenna is built on a low loss material. It has the ability to select a single frequency out of fifteen different bands and maintain the omnidirectional radiation pattern properties. Furthermore, the antenna is designed, built, and tested. Simulation and measurement results show that the antenna operates well at the specific frequency range. Therefore, the antenna is suitable to be used for switching frequencies in the band of TV, GSM900/1800, 3G, ISM 2.4 GHz, and above.

1. Introduction

Narrowband-to-narrowband frequency reconfiguration with harmonic suppression is currently preferred to support communication system, particularly wireless application, due to single type of this antenna that can reduce the size of the RF front-end electronic circuits. However, this type of antenna operates at one specific frequency at one time. Besides, the implementation of switch can cause additional loss and thus reduce antenna efficiency. It is noteworthy that high bandwidth tunable reconfigurable antenna has several advantages if used compared to the initial antenna geometry. In contrast, the existence of high frequency mode may interfere the system operation and will require filter circuit at the output. This in turn will raise the complexity of the terminal circuit and the overall size of system. This problem can be overcome by using the state of art of tunable reconfigurable antenna which is able to suppress harmonic frequencies. In addition, its compact size has attracted many antenna designers in recent years.

Recently, combining narrowband configuration to tunable narrowband in order to eliminate harmonic frequencies is a new approach. The combination of tunable frequency, harmonic suppression, and size reduction technique is very important and a key to construct the most optimum reconfigurable antenna. The use of fractal antenna can decrease the physical size of the antenna.

As far as harmonic suppressed antenna (HSA) with switch is concerned, the harmonic suppressed reconfigurable antennas have been published previously in the literature [1, 2]. The work on this type of antenna has been reported by using a linear dipole and log periodic dipole arrays, respectively. The first idea to create such antenna is presented in [1]. In a reconfigurable linear dipole in [1], 24 switches were used to control the antenna and the stub length. The antenna can change the operating frequency from a narrowband-to-narrowband features as well as suppress the harmonic frequency in the frequency range from 900 MHz to 3.5 GHz. However, this antenna is large due to the antenna itself as well as the tapered balun used. The latter has 28 switches [2]. The antenna can configure the operating frequency, that is, from wideband to narrowband, by switching ON and OFF the radiating elements. Ideal switches are also used to control each pair of dipole arm and to switch the related stub. In addition, the antenna can operate from 1 to 3 GHz and can be changed to other narrowband frequencies with large size.

Three antennas, namely, reconfigurable planar inverted-F antenna (RPIFA), reconfigurable ring patch antenna (RRPA),

Table 1: Reconfigurable printed antenna with ideal switches.

Reference	Antenna figure	Antenna structure	Switching band	Frequency switching technique	Switch types	Number of switches
[1]	Mirkamali et al. (2006) (University of Birmingham, UK)	Linear dipole	0.9 GHz, 1.05 GHz, 1.205 GHz, 1.460 GHz, 1.750 GHz, 2.05 GHz, and 2.770 GHz	Control effective radiating length	Metal patch (ideal switch)	24
[2]	Mirkamali et al. (2010) (University of Birmingham, UK)	Log periodic dipole	Mode 1: 1–3 GHz, Mode 2: 0.94 GHz, Mode 3: 1.217 GHz Mode 4: 1.477 GHz	Control effective radiating element	Metal patch (ideal switch)	28
[3]	Chamming (2003) (Virginia Polytechnic Institute & State University)	PIFA	1.48 GHz, 1.49 GHz, 1.5 GHz, 1.51 GHz, 1.53 GHz, and 1.51 GHz, and 1.54 GHz	Change the ground plane length	Metal patch (ideal switch)	12
		RRPA	1.50 GHz, 1.52 GHz, and 1.53 GHz	Control the ring width	Metal patch (ideal switch)	80
		RPFDA	0.94 GHz, 1.01 GHz, 1.03 GHz, 1.04 GHz, 1.05 GHz, and 1.12 GHz	Control the parasitic element length	Metal patch (ideal switch)	8
Proposed in this article	Hamzah et al. (2013) (Universiti Teknologi Malaysia, Malaysia)	Koch dipole	691 MHz, 725 MHz, 734 MHz, 865 MHz, 953 MHz, 987 MHz, 1099 MHz, 1160 MHz, 1190 MHz, 1270 MHz, 1440 MHz, 1650 MHz, 1880 MHz, 2350 MHz, and 3010 MHz	Control effective radiating length	Metal patch (ideal switch)	50

and reconfigurable folded parasitic dipole antenna (RPFDA) with switches have been proposed [3]. These antennas are integrated with 12, 80, and 8 switches, respectively. Through these published papers, the usage of ideal switches to demonstrate reconfigurable antennas is relevant. The features of antennas, that is, switching band, are tabulated and summarized in Table 1.

Reconfigurable antennas based on fractal shape have attracted many researchers in recent years. The antenna has many advantages such as large bandwidth, multifrequency and can reduce the antenna size. Koch and Hilbert curve as well as a Sierpinski Carpet are among the selected geometries to be studied for the antenna innovation. Many researchers have used these geometries in order to generate reconfigurable antenna that can configure the frequency or radiation pattern while exhibiting size reduction.

References [4–11] reported on reconfigurable fractal antennas. A Hilbert curve patch antenna uses six MEMS switches to configure the radiation pattern from 12.4 GHz to 12.65 GHz [4]. Four MEMS switches have been used in a Sierpinski gasket dipole to switch the frequency operation from 14 GHz (band 1) to 8 GHz and 25 GHz (band 2) [6]. Other studies on reconfigurable fractal antennas use Sierpinski gasket, Hilbert curve, and von Koch geometry [5, 7–11]. Three switches located at the radiating element are used to change the operating frequency at 620 MHz, 630 MHz, and 640 MHz [7]. Five states of operating frequencies in Sierpinski gasket's antenna are demonstrated by controlling the switches condition [8]. Twelve switches have been used to tune 60 GHz and 80 GHz in the Koch patch antenna [9]. Thirty switches have been used in three-dimensional fractal tree antennas to configure operating frequency from 770 MHz to 1570 MHz [10]. Six switches have been employed in Sierpinski gasket antenna to tune the frequency at 2.4 GHz, 5.7 GHz, 9.4 GHz, and 18 GHz [11]. Four switches are used to configure the radiation pattern at 8.4 GHz in a square patch fractal [5]. Some of them are summarized in Table 2.

Other published works on reconfigurable antenna are available in [12–17] which employed dipole antenna that is integrated with loop and open wire [12], U-Koch slotted monopole antenna [14], bow-tie antenna [15], UWB patch monopole antenna with spiral section [16], cedar-shaped fractal monopole antenna [17], and slotted monopole antenna (combination of square-ring and L-shaped linear) [13], respectively.

The work explained in this paper includes the research idea based on "harmonic suppressed frequency reconfigurable antenna" that can be obtained by controlling the radiation element length combined with internal filter. It is named as TMFDB25 antenna [18]. The balun circuit is reduced by 75% of height that made the antenna more practical. Moreover, the current is flowing directly through the terminal to the antenna input. The direction of current flow or current stop from the input terminal can be determined by means of open circuit stub placed at the terminal. An extensive simulation work has been carried out using two commercial software. The measurements are done using semianechoic chamber to validate the technique. The design consideration

Table 2: Reconfigurable fractal antenna.

Reference	Antenna structure	Number/type of switches	Comments
[10]	Sierpinski gasket	6/MEMS switch	Changing the frequency from 2.4 GHz, 5.7 GHz, and 9.4 GHz to 18 GHz
[6]	Sierpinski gasket	4/MEMS switch	Changing the frequency from 7 GHz, and 8 GHz, 14 GHz to 23 GHz
[9]	Fractal tree	204/copper strip (ideal switch)	Changing the frequency from 600 MHz to 1600 MHz (approximately 20 bands)
[7]	Hilbert curve	2/metal patch (ideal switch)	Changing the frequency from 620 GHz, 627 GHz to 635 GHz
[4]	Hilbert curve	8/metal patch (ideal switch)	Changing the pattern at $f = 9.0$ GHz
[8]	Koch Patch	18/copper strip (ideal switch)	Changing the pattern at 60 GHz and 80 GHz
[11]	Square fractal loop	4/metal patch (ideal switch)	Changing the pattern at $f = 8.4$ GHz
Proposed in this paper	TMFDB25	50/copper strip (ideal switch)	Changing the frequency from 600 MHz to 3.5 GHz with suppressed higher order mode

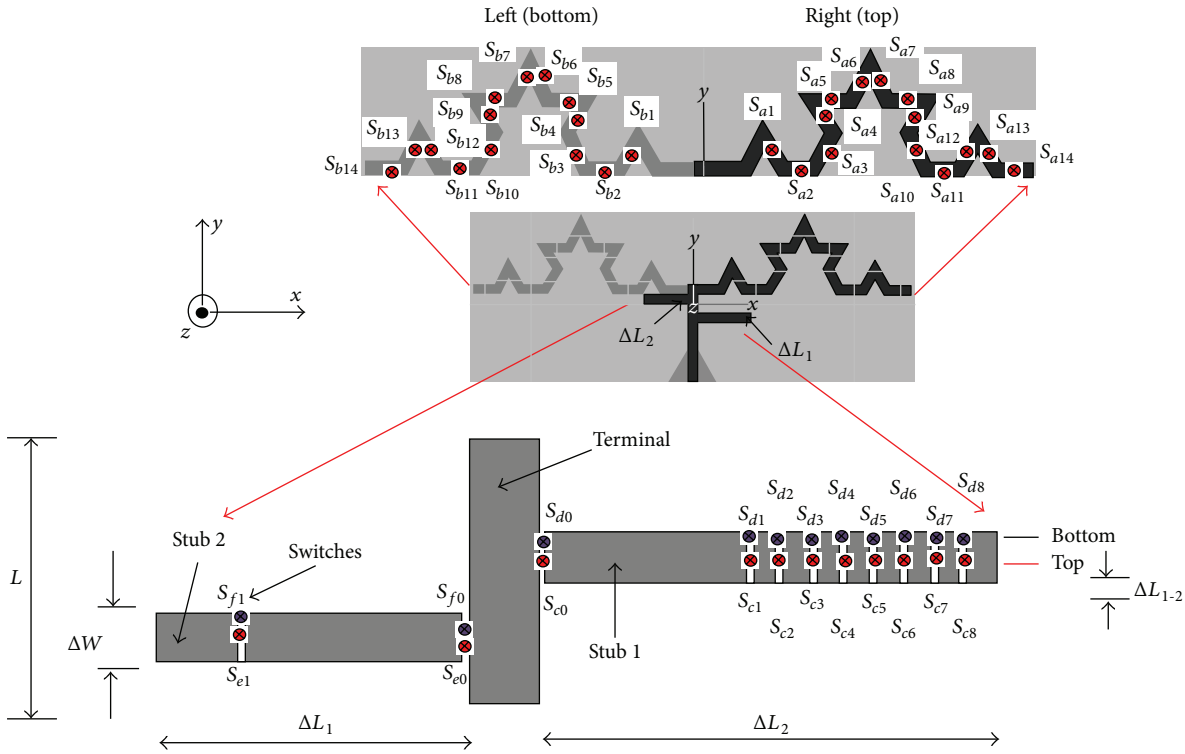

Figure 1: TMFDB25 antenna geometry.

is explained in Section 2 while all results are reported in Section 3. Finally, Section 4 concludes this paper.

2. TMFDB25 Antenna

The geometry of TMFDB25 is shown in Figure 1. The antenna is excited using microstrip line with small tapered balun (75% size reduction) by an SMA connector. The antenna consists of a radiating element, stubs and terminal, tapered balun, and switches. Furthermore, the Koch curve is used to minimize the antenna size, while the double-sided structure is selected due to the ability to lock in the harmonic frequency. Figure 1 shows the geometrical layout of the antenna with a gap (slot) which acts as a switch. The slot size of 1.0 mm × 1.5 mm is used to change the radiating element length as well as the stubs. For achieving reconfigurable capability, the antennas need to be able to change its length to resonate at the desired frequencies. In this design the elimination of higher order mode is considered and controlled via the implementation of open circuit stubs as presented in the figure. The antenna dipole arm is connected with 28 switches while 22 switches are used at the stubs to realize the reconfigurable antenna with harmonic suppression capability.

Table 3: Switch configuration states for different length of radiating element. Units are in mm.

Length (x-axis)	Switch conditions (left arm)	Switch conditions (right arm)	MFDB25 Stub 1, Stub 2	Band
137	Sa1 to Sa14 are ON	Sb1 to Sb14 are ON	(37, 24)	Band 1
128	Sa2 to Sa14 are ON	S2b to Sb14 are ON	(36, 23)	Band 2
120	Sa3 to Sa14 are ON	S3b to Sb14 are ON	(34, 0)	Band 3
112	Sa4 to Sa14 are ON	Sb4 to Sb14 are ON	(32, 0)	Band 4
104	Sa5 to Sa14 are ON	Sb5 to Sb14 are ON	(30, 0)	Band 5
96	Sa6 to Sa14 are ON	Sb6 to Sb14 are ON	(27, 0)	Band 6
88	Sa7 to Sa14 are ON	Sb7 to Sb14 are ON	(25, 0)	Band 7
84	Sa8 to Sa14 are ON	Sb8 to Sb14 are ON	(23, 0)	Band 8
76	Sa9 to Sa14 are ON	Sb9 to Sb14 are ON	(22, 0)	Band 9
66	Sa10 to Sa14 are ON	Sb10 to Sb14 are ON	Not used	Band 10
60	Sa11 to Sa14 are ON	Sb11 to Sb14 are ON	Not used	Band 11
52	Sa12 to Sa14 are ON	Sb12 to Sb14 are ON	Not used	Band 12
44	Sa13 to Sa14 are ON	Sb13 to Sb14 are ON	Not used	Band 13
36	Sa14 is ON	Sb14 is ON	Not used	Band 14
28	All switches are OFF	All switches are OFF	Not used	Band 15

Table 4: Effect of terminal length, L, on resonance in Figure 1.

Resonance	L_1, mm	L_2, mm	L_3, mm	L_4, mm	L_5, mm	L_6, mm	L_7, mm
	10	12	14	16	18	20	22
f (GHz), dB	0.74, −23	0.74, −24	0.74, −25	0.74, −26	0.74, −27	0.74, −28	0.74, −29
1st HM (GHz), dB	2.02, −1.6	1.98, −3	1.98, −3	1.99, −3	1.99, −3	1.99, −3	1.99, −3
2nd HM (GHz), dB	2.79, −1.8	2.27, −4	2.28, −4	2.28, −4	2.28, −3	2.28, −3	2.28, −3

Table 5: Effect of stubfilter's length on resonance in Figure 1 is location of stub 2 with respect to stub 1.

Resonance	$\Delta L_{1\text{-}2}$, mm						
	0	1	2	3	4	5	6
f (GHz), dB	0.74, −22	0.74, −29	0.74, −23	0.74, −23	0.74, −27	0.74, −24	0.74, −23
1st HM (GHz), dB	2.36, −31	2, −2	1.99, −3	1.98, −3	1.98, −5	1.96, −7	1.94, −12
2nd HM (GHz), dB	NA	2.36, −13	2.29, −6	2.25, −2	NA	NA	NA

In this design conceptual, the frequency reconfiguration totally depends on the radiating element length while stubs 1, 2 suppressed their corresponding higher order modes. It can be observed in the figure that the length, ΔL, of the antenna in x-axis is approximately quarter wavelength of 740 MHz. Switches Sa1, Sa2, ..., Sa8 and Sb1, Sb2, ..., Sb8 located at specific positions are used to switch the operating frequencies, while Sc0Sd0, Sc1Sd1, ..., Sc8Sd8 and Se0Sf0 to Se1Sf1 are used to shorten the antenna. The switches Sc and Sd are connected in parallel to join each part of stub 1 while the Se and Sf switches for stub 2. When the antenna operates at 740 MHz, it has two higher order modes operating at 2020 MHz and 3020 MHz. At the moment, all switches are ON (as shown in Figure 1) to allow the antenna radiate at this frequency and at the same time suppress the higher order mode. It should be noted that the stubs have mismatched the antenna at the higher order mode and the concept is extended to other operating frequencies from 400 MHz to 3.5 GHz. The band, switches condition, and the stub length are tabulated in Table 3.

Besides that, the terminal length, stub width, and stubs location need to be optimized for better performance. These parameters can provide sufficiently small reflections and avoid the appearance of undesired higher order modes. The configuration is proposed since it exhibits omnidirectional radiation pattern with low level of cross-polarization, as well as it can suppress higher order modes, although with a simple structure. The fractal technology applied allows minimization of the antenna size. Open circuit stub has been used to trap the higher order mode that acts as stubfilters. This antenna is simulated using numerical simulations and cross-checked by using the finite element method- (FEM-) based simulations.

The measured results of the return loss of Figure 1 are presented in Figure 2. Good agreement is observed between the results obtained using commercial software and measurement. They operate at these particular bands which directly depend on the switches states. The corresponding resonant frequency is also given in the figure.

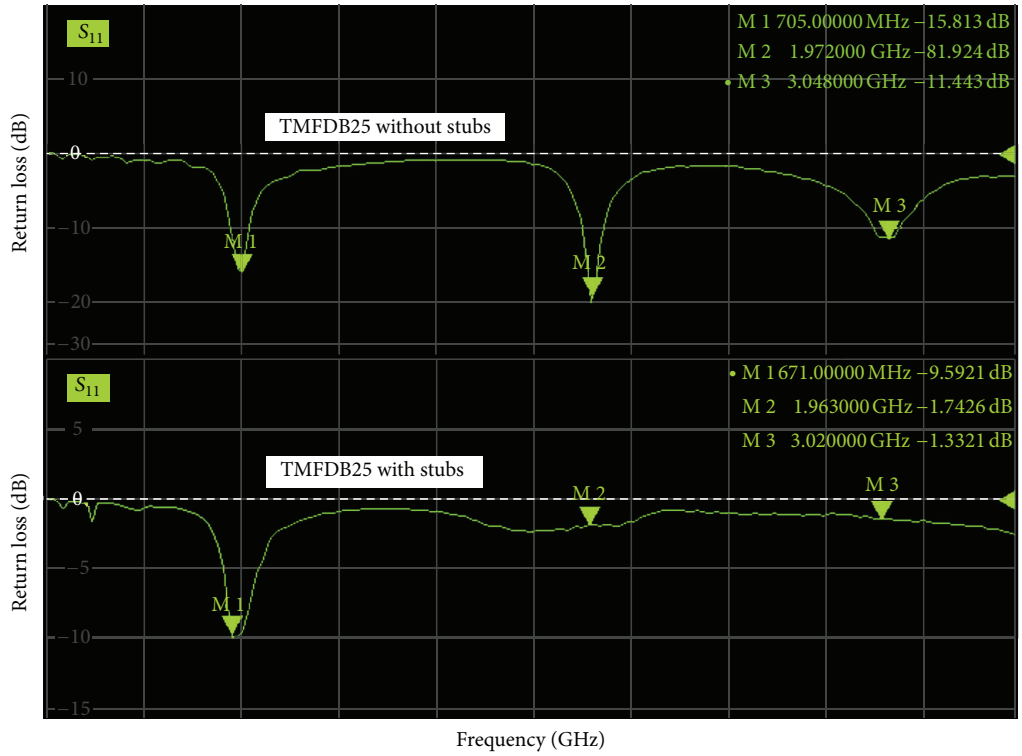

Figure 2: Measured return losses of the TMFDB25 antenna at two conditions: (1) TMFDB25 without stubs and (2) TMFDB25 with stubs 1, 2. In this study, f equals 705 MHz while 1st HM = 1.972 GHz and 2nd HM = 3.048 GHz, and suppressed return losses of 1st HM and 2nd HM equals −1.7429 dB and −1.3321 dB, respectively.

Table 6: Effect of stubfilter's width on resonance in Figure 1.

Resonance	ΔW_3, mm 1.0	ΔW_4, mm 1.5	ΔW_5, mm 2.0	ΔW_6, mm 2.5	ΔW_7, mm 3.0	ΔW_8, mm 3.5	ΔW_9, mm 4.0
f (GHz), dB	0.74, −25	0.74, −29	0.74, −36	0.74, −25	0.74, −23	0.74, −19	0.74, −17
1st HM (GHz), dB	1.99, −4	1.99, −4	1.99, −4	1.98, −3	2.02, −1.6	1.99, −3	1.98, −3
2nd HM (GHz), dB	2.35, −13	2.33, −9	2.3, −7	2.27, −5	2.79, −1.8	2.27, −2	2.27, −1.4

Table 7: Return losses and VSWR results of theoretical predictions versus measurement for TMFDB25 antenna.

Band	Return loss						VSWR		
	CST		HFSS		Measured		CST	HFSS	Measured
Band 1	745 MHz	−14.4 dB	733 MHz	−25.3784 dB	691 MHz	−12.5 dB	1.468	1.14900	1.5856
Band 2	766 MHz	−16.4 dB	754 MHz	−23.5454 dB	720 MHz	−17.0 dB	1.358	1.12704	1.4373
Band 3	801 MHz	−34.0 dB	796 MHz	−23.5129 dB	725 MHz	−24.5 dB	1.041	1.14301	1.1157
Band 4	843 MHz	−36.8 dB	838 MHz	−23.1433 dB	734 MHz	−35.0 dB	1.030	1.14969	1.0360
Band 5	903 MHz	−39.6 dB	897.5 MHz	−23.6867 dB	865 MHz	−17.0 dB	1.022	1.13998	1.4367
Band 6	969 MHz	−39.5 dB	960.5 MHz	−27.2084 dB	953 MHz	−20.0 dB	1.021	1.09119	1.3403
Band 7	1029 MHz	−31.4 dB	1020 MHz	−29.0275 dB	987 MHz	−15.0 dB	1.055	1.07333	1.4221
Band 8	1099 MHz	−29.1 dB	1104 MHz	−27.9649 dB	1160 MHz	−27.0 dB	1.099	1.08327	1.2220
Band 9	1190 MHz	−27.3 dB	1195 MHz	−26.5608 dB	1250 MHz	−19.5 dB	1.090	1.09860	1.3705
Band 10	1270 MHz	−20.5 dB	1282.5 MHz	−15.8776 dB	1270 MHz	−16.5 dB	1.210	1.38304	1.3993
Band 11	1428 MHz	−23.9 dB	1429.5 MHz	−17.1505 dB	1440 MHz	−16.5 dB	1.136	1.32241	1.3863
Band 12	1596 MHz	−47.0 dB	1597.5 MHz	−22.3475 dB	1650 MHz	−18.0 dB	1.009	1.16524	1.2535
Band 13	1879 MHz	−30.3 dB	1916 MHz	−45.262 dB	1880 MHz	−19.5 dB	1.063	1.01097	1.2723
Band 14	2345 MHz	−32.4 dB	2458.5 MHz	−18.946 dB	2350 MHz	−18.0 dB	1.049	1.25454	1.2737
Band 15	2922 MHz	−34.5 dB	3074 MHz	−18.4166 dB	3010 MHz	−40.0 dB	1.039	1.27271	1.0207

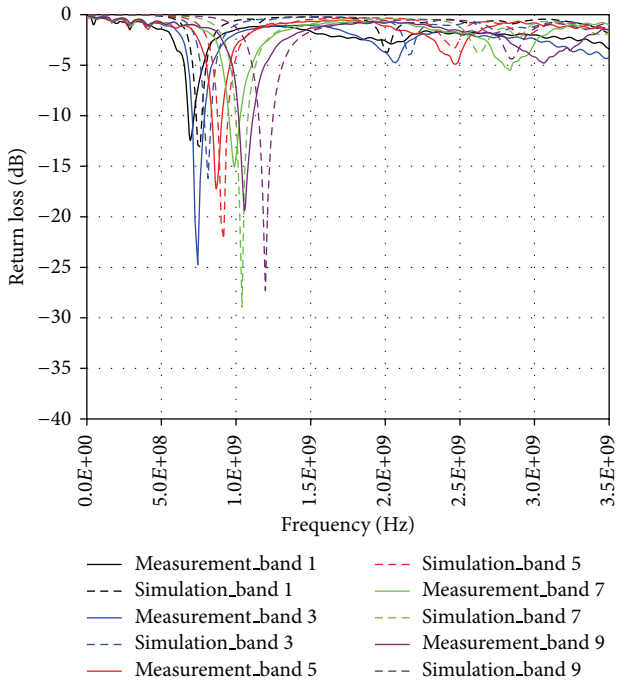

Figure 3: Simulated and measured return losses at Bands 1, 3, 5, 7, and 9.

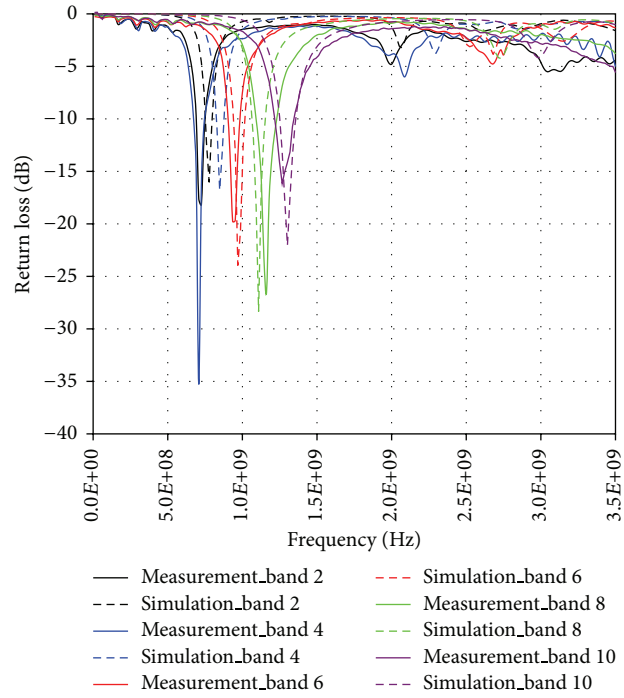

Figure 4: Simulated and measured return losses at Bands 2, 4, 6, 8, and 10.

3. Results and Discussion

3.1. Antenna Optimization-Parametric Study. In this section, three important antenna parameters in Figure 1 which are the terminal length, L, distance between stubs, $\Delta L_{1\text{-}2}$, and the stub's widths, ΔW, are studied. By means of varying these parameters in uniform increment, the following data are obtained. The effect of the operating frequency, 1st HM and 2nd HM are observed as shown in the table.

Table 4 tabulates the simulated resonance frequency for antenna when the antenna terminal length is changed from 10 mm to 22 mm. Results show that the antenna resonates at 740 MHz in the range from 0 to 3.5 GHz with different return losses. When the terminal length is increased, a better return loss is achieved, whereby this action brings the line impedance value to the point closer to the characteristic impedance. The 10 mm length is selected due to its smaller size.

Cautious steps are taken to ensure the investigation is valid. The effect of stub location is highlighted in Table 5. Actual length of the antenna terminal is approximately 8 mm. The variation starts from 0 mm to 6 mm with an increment of 1 mm each. It is shown that the antenna can maintain the resonant frequency at 740 MHz with excellent return loss of < -20 dB although the stub location is varied. The stub location of 3 mm totally rejected the higher order mode. However, there is harmonic frequency for certain conditions.

Table 6 tabulates the resonance frequency for antenna when the stub width is changed from 1 mm to 4 mm. The antenna has first resonance at 740 MHz with different return losses for all cases. The width of 3 mm totally rejected the harmonic frequencies and has good return loss of −23 dB for the operating frequency. These optimum parameters have been used in the designing of the TMFDB25 antenna.

3.2. TMFDB25 Antenna. Basically, the proposed antenna is constructed by measuring its electrical properties in order to verify the theoretical and simulation results. The selection of this antenna to be developed is based on small size upon optimization and excellent performance. To achieve fifteen-band TMFDB25 antenna, a small strip of copper is used as the substitute for the RF switches. Then, to be a fifteen-band TMFDB25 antenna with suppressed higher order modes, the stubs are connected. They enlarged the number of small strips of copper. The latter is soldered to the radiating element as well as the stub sections at the switch locations to simulate the switch ON states. The copper strips are made from the standard copper tape and are approximately 0.2 mm wide. The tape switches are sufficiently long enough (2 mm) to both span the 1 mm gap separating the radiating element and the stub length. It provides enough metal-to-metal contact for good solder joint. In addition, for good presentation, the switch has been labeled as black colour for ON states and a cross-line (red colour) for OFF states.

The corresponding measured results of the return loss are depicted in Figures 3 to 5. It should be noted that this research work is very challenging and requires huge amount of measurement period. However, they are successful to be plotted. The huge numbers of switches have been used and hence increase the difficulty to suppress the higher order modes.

Then the measured results are compared with the simulation works. It can be seen in Figure 3 that the designed

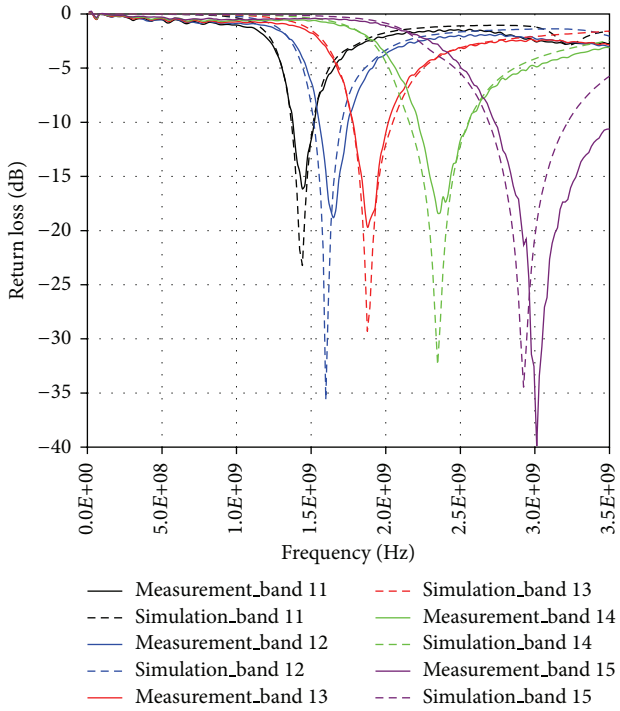

FIGURE 5: Simulated and measured return losses at bands 10, 11, 12, 13, 14, and 15.

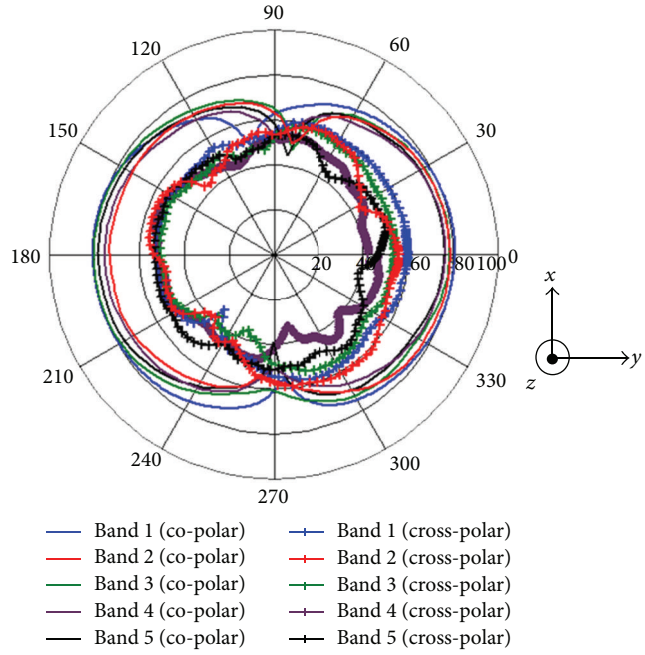

FIGURE 6: Measured E-plane radiation patterns (co-polar & cross-polar) at operating frequency, f, for TMFDB25 with stubs 1, 2 at bands 1 to 5.

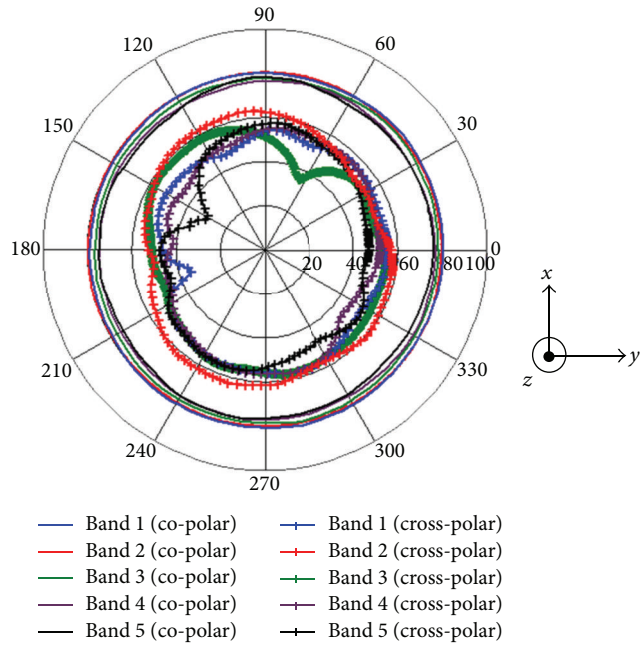

FIGURE 7: Measured H-plane radiation patterns (co-polar & cross-polar) at operating frequency, f, for TMFDB25 with stubs 1, 2 at bands 1 to 5.

antenna can be tuned from band 1 = 691 MHz, band 3 = 725 MHz, band 5 = 865 MHz, band 7 = 987 MHz, and band 9 = 1270 MHz while the simulated are band 1 = 745 MHz, band 3 = 801 MHz, band 5 = 903 MHz, band 7 = 1029 MHz, and band 9 = 1190 MHz at a time.

It can also be observed in Figure 4 that the antenna can be tuned from bands 2, 4, 6, 8, and 10 with suppressed higher modes. In this case, the measurements are band 2 = 725 MHz, band 4 = 734 MHz, band 6 = 953 MHz, band 8 = 1160 MHz, and band 10 = 1270 MHz while the simulated are band 2 = 766 MHz, band 4 = 843 MHz, band 6 = 969 MHz, band 8 = 1099 MHz, and band 10 = 1270 MHz.

Then, in Figure 5, the antenna tuned the bands from bands 11, 12, 13, 14, and 15 with suppressed higher modes. (Measured: band 11 = 1440 MHz, band 12 = 1650 MHz, band 13 = 1880 MHz, band 14 = 2350 MHz, and band 15 = 3010 MHz while the simulated are band 11 = 1428 MHz, band 12 = 1596 MHz, band 13 = 1879 MHz, band 14 = 2345 MHz, and band 15 = 2922 MHz). The bandwidth covering tunable ranges are obtained as 1659 MHz. The corresponding measured return losses are −12.5 dB (band 1), −17 dB (band 2), −24.5 dB (band 3), −35 dB (band 4), −17 dB (band 5), −20 dB (band 6), −31.4 dB (band 7), −27 dB (band 8), −27.3 dB (band 9), −16.5 dB (band 10), −16.5 dB (band 11), −18 dB (band 12), −19.5 dB (band 13), −18.0 dB (band 14), and −34.5 dB (band 15).

The simulation of the operating frequencies (bands 1, 2, and 3 to 15) of the TMFDB25 antenna with stubs has been done using CST code and HFSS code (not shown in this paper due to limited number of pages).

Table 7 presents the simulated (CST code and HFSS code) and measured return losses and corresponding VSWR performances of the TMFDB25 antenna for each band. The antenna can be tuned to a single frequency at a time as tabulated in the table. The stubs have effectively reduced the input

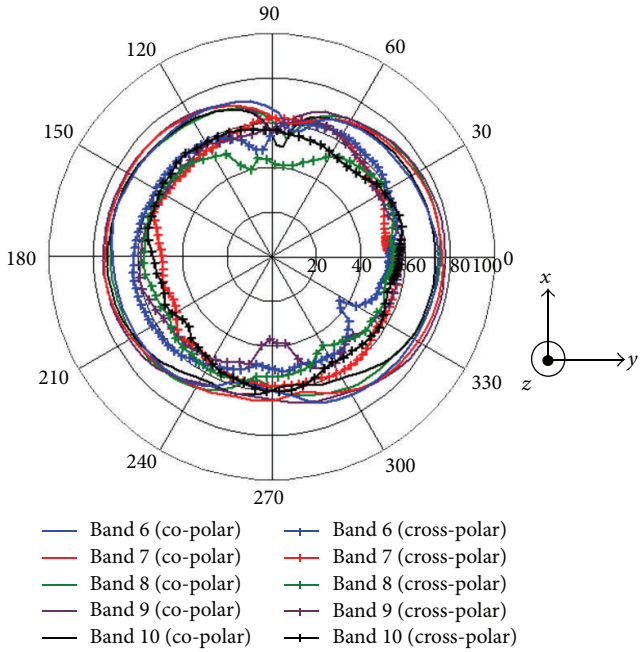

Figure 8: Measured E-plane radiation patterns (co-polar & cross-polar) at operating frequency, f, for TMFDB25 with stubs 1, 2 at bands 6 to 10.

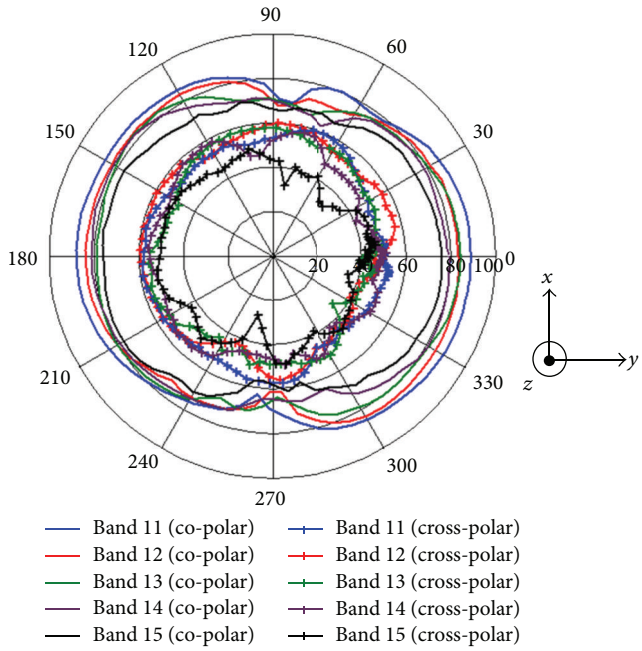

Figure 10: Measured E-Plane radiation patterns (co-polar & cross-polar) at operating frequency, f, for TMFDB25 with stubs 1, 2 at bands 11 to 15.

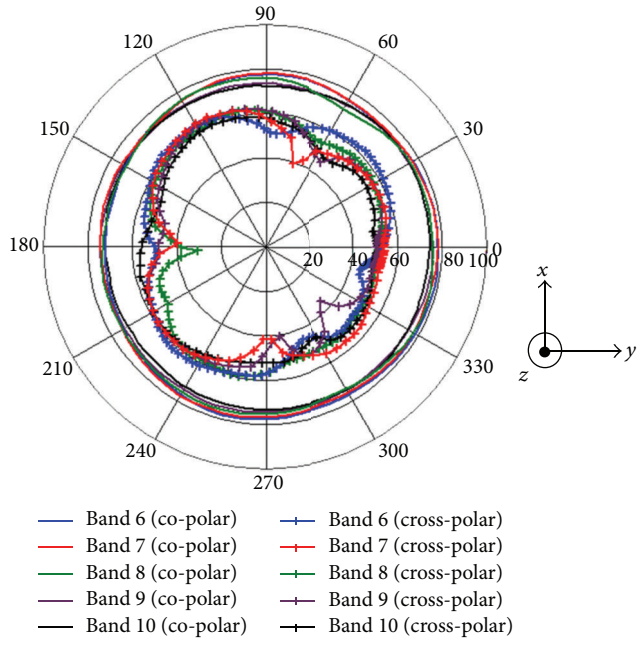

Figure 9: Measured H-plane radiation patterns (co-polar & cross-polar) at operating frequency, f, for TMFDB25 with stubs 1, 2 at bands 6 to 10.

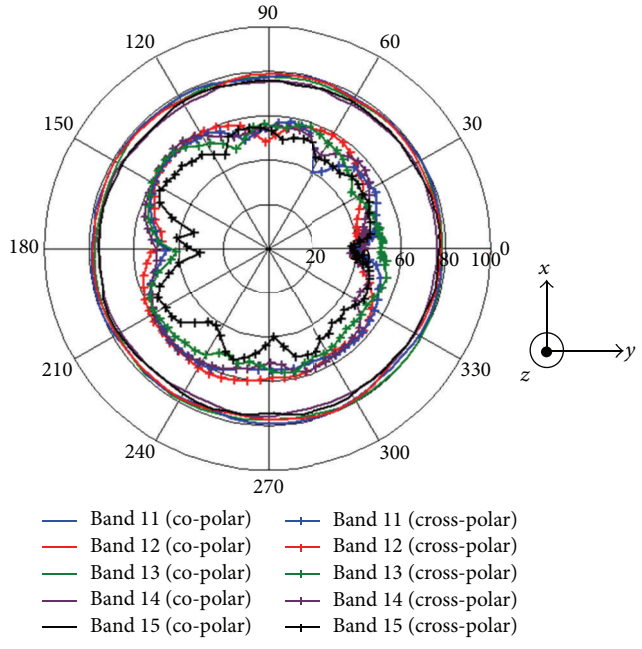

Figure 11: Measured H-plane radiation patterns (co-polar & cross-polar) at operating frequency, f, for TMFDB25 with stubs 1, 2 at bands 10 to 15.

reflections and thus corresponding VSWRs. Channel operating bandwidths is obtained by CST, HFSS, and measurements are 2177 MHz, 2341 MHz, and 2319 MHz, respectively. Good agreement is observed for the measurement and simulation results in terms of operating frequencies, return losses, and VSWRs. The main factor that contributes to the measurement results is a little bit different compared to the simulation data due to the imperfect work during soldering of the copper to join each stub segment.

In this study, the corresponding measured E-plane and H-plane radiation patterns at the operating frequencies in Figures 3 to 5 are presented in Figures 6, 7, 8, 9, 10, and

11, respectively. These figures provide the H-plane (x-z axis) and the E-plane (z-x axis) patterns for bands 1 to 15. In this work, it is found that the pattern behavior for the fifteen bands antenna resembles that of a simple dipole antenna. The patterns are closed to omnidirectional in the H-plane, having a figure-of-eight pattern in the E-plane.

As predicted by the simulations, the radiation patterns of most bands remain nearly constant from one switch state to the next. This situation is desired for the antenna in order to maintain the performance while selecting the operating frequency. This consistency can be clearly seen in the pattern comparison of bands 1 to 15.

4. Conclusion

TMFDB25 antenna with harmonic suppression capability that is suitable for frequency reconfiguration in the frequency bands of TV (400 MHz–800 MHz), GSM900/1800 MHz, 3G, ISM 2.4 GHz, and above (up to 3.5 GHz) is presented. The TMFDB25 is an improvement on the conventional linear dipole antenna with harmonic suppressed behavior. A total of 50 RF switch locations were incorporated into the design to achieve the desired frequency reconfigurable performance. Single operating frequency out of fifteen bands can be selected by changing the antenna's length, and the stub is used to suppress the harmonic frequency. The proposed TMFDB25 antenna has a practical size with 51.8% size reduction compared to the reference [1]. The corresponding measured return loss and VSWR are found to be in good agreement with the computed performances. The simulated and measured data demonstrate that the antenna indeed provides the desired wideband frequency reconfiguration. The number of operating frequency can be increased by increasing the number of switches. In addition, an omniradiation pattern is maintained for the whole frequency. The performance verifies the proposed design concept. From the simulation and experimental results, it can be concluded that the proposed antennas have a unique structure compared to the available published "harmonic suppressed reconfigurable antenna" or "reconfigurable fractal antenna."

Acknowledgments

The work is supported by Universiti Teknologi Malaysia, Research University Grant vote 04J25 and PY/2012/01578, and Ministry of Education Malaysia, Fundamental Research Grant Scheme vote 4F039. The authors are grateful to Universiti Tun Hussein Onn Malaysia for supporting PhD studies of S. A. Hamzah. Simulations were done at the Radio Communication and Antenna Design Laboratory (RACAD), UTHM. Measurements were performed at EMC centre, UTHM.

References

[1] A. Mirkamali, P. S. Hall, and M. Soleimani, "Reconfigurable printed-dipole antenna with harmonic trap for wideband applications," *Microwave and Optical Technology Letters*, vol. 48, no. 5, pp. 927–929, 2006.

[2] A. Mirkamali, P. S. Hall, and M. Soleiman, "Wideband frequency reconfiguration of a printed log periodic dipole array," *Microwave and Optical Technology Letters*, vol. 52, no. 4, pp. 861–864, 2010.

[3] N. P. Chamming, *Active antenna bandwidth control using reconfigurable antenna elements [Ph.D. thesis]*, Virginia Polytechnic Institute & State University, 2003.

[4] X.-S. Yang, B.-Z. Wang, and Y. Zhang, "A reconfigurable Hilbert curve patch antenna," in *Proceedings of the IEEE Antennas and Propagation Society International Symposium and USNC/URSI Meeting*, pp. 613–616, July 2005.

[5] W. Wu, B.-Z. Wang, X.-S. Yang, and Y. Zhang, "A pattern-reconfigurable planar fractal antenna and its characteristic-mode analysis," *IEEE Antennas and Propagation Magazine*, vol. 49, no. 3, pp. 68–75, 2007.

[6] Y. Zhang, B.-Z. Wang, and X.-S. Yang, "Fractal Hilbert microstrip antennas with reconfigurable radiation patterns," *Microwave and Optical Technology Letters*, vol. 49, no. 2, pp. 352–354, 2007.

[7] D. E. Anagnostou, G. Zheng, M. T. Chryssomallis et al., "Design, fabrication, and measurements of an RF-MEMS-based self-similar reconfigurable antenna," *IEEE Transactions on Antennas and Propagation*, vol. 54, no. 2, pp. 422–432, 2006.

[8] K. J. Vinoy and V. K. Varadan, "Design of reconfigurable fractal antennas and RF MEMS for space based system," *Optical Engineering*, vol. 4591, pp. 185–196, 2001.

[9] H. Lui, B. Z. Wang, and W. Shao, "Dual band bi-directional pattern reconfigurable fractal patch antenna for milimeter wave application," *International Journal of Infrared and Millimeter Waves*, vol. 28, no. 1, pp. 25–31, 2007.

[10] J. S. Petko and D. H. Werner, "Miniature reconfigurable three-dimensional fractal tree antennas," *IEEE Transactions on Antennas and Propagation*, vol. 52, no. 8, pp. 1945–1956, 2004.

[11] N. Kingsley, D. E. Anagnostou, M. M. Tentzeris, and J. Papapolymerou, "RF MEMS sequentially reconfigurable sierpinski antenna on a flexible organic substrate with novel DC-biasing technique," *Journal of Microelectromechanical Systems*, vol. 16, no. 5, pp. 1185–1192, 2007.

[12] W. Kang, K. H. Ko, and K. Kim, "A compact beam reconfigurable antenna for symmetric beam switching," *Progress In Electromagnetics Research*, vol. 129, pp. 1–16, 2012.

[13] C. C. Wang, L. T. Chen, and J. S. Row, "Reconfigurable Slot antenna with circular polarization," *Progress In Electromagnetics Research*, vol. 34, pp. 101–110, 2012.

[14] A. H. Ramadan, K. Y. Kabalan, A. El-Hajj, S. Khoury, and M. Al-Husseini, "A reconfigurable U-Koch microstrip antenna for wireless applications," *Progress in Electromagnetics Research*, vol. 93, pp. 355–367, 2009.

[15] N. Romano, G. Prisco, and F. Soldovieri, "Design of a reconfigurable antenna for ground penetrating radar applications," *Progress in Electromagnetics Research*, vol. 94, pp. 1–18, 2009.

[16] S. Manafi, S. Nikmehr, and M. Bemani, "A planar reconfigurable multifunctional antenna for WLAN/WiMAX/UWB/PCS-DCS/UMTS applications," *Progress In Electromagnetics Research C*, vol. 26, pp. 123–137, 2012.

[17] M. Al-Husseini, M. A. Madi, A. H. Ramadan, K. Y. Kabalan, and A. El-Hajj, "A reconfigurable cedar-shaped microstrip antenna for wireless applications," *Progress In Electromagnetics Research C*, vol. 25, pp. 209–221, 2011.

[18] S. A. Hamzah and M. Esa, "Miniaturized single band microwave fractal dipole antenna and its tunable configuration," in *Proceedings of the of IEEE APS*, pp. 1–4, July 2010.